

Manipulation of the Majorana Ising spin via Rashba-Dresselhaus spin-orbit coupling

Lili Liu(刘利利), Qi-Sheng Xu(徐其胜), Cai Chen(陈才), Chui-Zhen Chen(陈垂针), and Dong-Hui Xu(许东辉)
Citation: Chin. Phys. B, 2026, 35 (**6**): 067404. DOI: 10.1088/1674-1056/ae43cd
http://cpb.iphy.ac.cn; http://iopscience.iop.org/cpb

What follows is a list of articles you may be interested in

Manipulation of vortex array via a magnetism-tunable spin-polarized scanning tunnelling microscopy

Bing Xia(夏冰), Hong-Yuan Chen(陈虹源), Jian Zheng(郑健), Bo Yang(杨波), Jie Cai(蔡杰), Yi Zhang(章毅), Yi Yang(杨毅), Hao Yang(杨浩), Dan-Dan Guan(管丹丹), Xiao-Xue Liu(刘晓雪), Liang Liu(刘亮), Yao-Yi Li(李耀义), Shi-Yong Wang(王世勇), Can-Hua Liu(刘灿华), Hao Zheng(郑浩), and Jin-Feng Jia(贾金锋)
Chin. Phys. B, 2025, 34 (**3**): 037402. DOI: 10.1088/1674-1056/adb38d

Customizing topological phases in the twisted bilayer superconductors with even-parity pairings

Conghao Lin(林丛豪), Chuanshuai Huang(黄传帅), and Xiancong Lu(卢仙聪)
Chin. Phys. B, 2023, 32 (**8**): 087401. DOI: 10.1088/1674-1056/acd3e3

Majorana zero modes induced by skyrmion lattice

Dong-Yang Jing(靖东洋), Huan-Yu Wang(王寰宇), Wen-Xiang Guo(郭文祥), and Wu-Ming Liu(刘伍明)
Chin. Phys. B, 2023, 32 (**1**): 017401. DOI: 10.1088/1674-1056/ac6ee7

Ac Josephson effect in Corbino-geometry Josephson junctions constructed on Bi_2Te_3 surface

Yunxiao Zhang(张云潇), Zhaozheng Lyu(吕昭征), Xiang Wang(王翔), Enna Zhuo(卓恩娜), Xiaopei Sun(孙晓培), Bing Li(李冰), Jie Shen(沈洁), Guangtong Liu(刘广同), Fanming Qu(屈凡明), and Li Lü(吕力)
Chin. Phys. B, 2022, 31 (**10**): 107402. DOI: 10.1088/1674-1056/ac89d4

Topological superconductivity in a $Bi_2Te_3/NbSe_2$ heterostructure: A review

Hao Zheng(郑浩), Jin-Feng Jia(贾金锋)
Chin. Phys. B, 2019, 28 (**6**): 067403. DOI: 10.1088/1674-1056/28/6/067403

SPECIAL TOPIC — Two-dimensional superconductivity

Manipulation of the Majorana Ising spin via Rashba–Dresselhaus spin–orbit coupling

Lili Liu(刘利利)[1,2,†,‡], Qi-Sheng Xu(徐其胜)[2,†], Cai Chen(陈才)[3], Chui-Zhen Chen(陈垂针)[4,§], and Dong-Hui Xu(许东辉)[2,5,¶]

[1] *College of Teacher Education, Chongqing Three Gorges University, Chongqing* 404100, *China*
[2] *Department of Physics and Chongqing Key Laboratory for Strongly Coupled Physics, Chongqing University, Chongqing* 400044, *China*
[3] *School of Civil Engineering, Chongqing Three Gorges University, Chongqing* 404100, *China*
[4] *Institute for Advanced Study and School of Physical Science and Technology, Soochow University, Suzhou* 215006, *China*
[5] *Center of Quantum Materials and Devices, Chongqing University, Chongqing* 400044, *China*

(Received 14 December 2025; revised manuscript received 28 January 2026; accepted manuscript online 10 February 2026)

Majorana surface states in time-reversal invariant (TRI) topological superconductors (TSCs) typically exhibit a highly anisotropic magnetic response, a phenomenon termed "Majorana Ising spins." This Ising character is governed by the crystalline symmetries protecting the topological phase. In this work, we investigate the orientation and tunability of Majorana Ising spins within TRI TSCs engineered in two-dimensional spin–orbit coupled systems proximitized to an extended s-wave superconductor. We demonstrate that the interplay between Rashba and Dresselhaus spin–orbit couplings (SOC) plays a decisive role in determining the Ising spin orientation. In the limit of pure Rashba SOC, the Ising spin aligns along the x-axis, protected by mirror symmetry M_x, whereas for pure Dresselhaus SOC, it orients along the y-axis, protected by the rotational symmetry C_{2y}. Crucially, we reveal that when both Rashba and Dresselhaus interactions coexist, the Ising spin direction becomes continuously tunable within the basal plane. By adjusting the relative strengths of the SOC parameters — experimentally accessible via gating in semiconductor heterostructures — any orientation between the x- and y axes can be achieved. We validate these findings by calculating the topological winding number W and elucidating the symmetry-protection mechanism for the tunable phases. Our results propose a pathway for manipulating Majorana fermions in quantum devices through purely electrical means, bridging the gap between symmetry-protected topology and functional spintronic applications.

Keywords: topological superconductors, Majorana zero modes, Majorana Ising spin

PACS: 74.25.–q, 74.78.Na

DOI: 10.1088/1674-1056/ae43cd **CSTR:** 32038.14.CPB.ae43cd

1. Introduction

The discovery of topological phases of matter has revolutionized our understanding of condensed matter physics, marking a paradigm shift from the classification of phases via local order parameters associated with symmetry breaking to the identification of global invariants that characterize the topology of the quantum wavefunction.[1] This topological classification, initially solidified by the discovery of topological insulators, has since expanded to include superconducting systems.[2] Among these, topological superconductors (TSCs) have garnered intense theoretical and experimental interest due to their potential to host Majorana fermions (MFs) — exotic quasiparticles that act as their own antiparticles and obey non-Abelian braiding statistics.[3] These properties render MFs promising candidates for the realization of fault-tolerant topological quantum computing, where quantum information is encoded non-locally in the parity of separated Majorana modes, protecting it from local decoherence sources.[4]

While the initial search for MFs predominantly focused on chiral p-wave superconductors and systems with broken time-reversal symmetry (TRS),[6,8] such as those in the Altland–Zirnbauer class D,[5,7] recent attention has shifted significantly toward time-reversal invariant (TRI) topological superconductors belonging to class DIII.[7] Class D systems are characterized by a $\mathbb{Z}_2$ or $\mathbb{Z}$ invariant depending on dimensionality, but they require substantial magnetic fields to break TRS, which can be detrimental to the parent superconducting state. In contrast, class DIII systems preserve TRS and are characterized by a $\mathbb{Z}_2$ invariant in one dimension and a $\mathbb{Z}$ invariant in two dimensions.

In class DIII systems, Kramers' theorem dictates that Majorana surface states must appear in pairs, commonly referred

[†]These authors contributed equally to this work.
[‡]Corresponding author. E-mail: liulili0612@163.com
[§]Corresponding author. E-mail: czchen@suda.edu.cn
[¶]Corresponding author. E-mail: donghuixu@cqu.edu.cn

© 2026 Chinese Physical Society and IOP Publishing Ltd. All rights, including for text and data mining, AI training, and similar technologies, are reserved.

to as Majorana Kramers pairs (MKPs). Unlike their chiral counterparts in class D, which are robust against any local perturbation preserving particle–hole symmetry, MKPs are protected by time-reversal symmetry. However, this protection is subtle; while a single MKP is robust against non-magnetic disorder, it can be gapped out by perturbations that break TRS, such as external magnetic fields. Crucially, protection is also afforded by additional crystalline symmetries of the host lattice. A defining, yet frequently overlooked, feature of these states is their anisotropic magnetic response.

Early phenomenological studies on the ^{3}He-B superfluid phase — a definitive 3D class DIII system — revealed highly anisotropic responses of its Majorana boundary states to external magnetic fields, detected through measurements of superconducting spin susceptibility and spin relaxation.[9,10] Researchers observed that the spin density operator for these surface states exhibited Ising-type behavior, with a distinct polarization axis often perpendicular to the surface. This implies that the Majorana modes remain gapless for magnetic fields applied perpendicular to this "Ising" axis but acquire a mass (gap) for fields parallel to it.[9,10,13,14,16] This anisotropic behavior led to the concept of the "Majorana Ising spin." Contemporaneous research established that in noncentrosymmetric topological superconductors, even when TRS is broken (rendering the strict $\mathbb{Z}_2$ classification formally invalid), a weak magnetic field applied perpendicular to the edge propagation direction could preserve the gapless nature of Majorana modes. This stability was attributed to accidental symmetries inherent to specific Hamiltonians, such as the Rashba spin–orbital coupled model.[12,17] Later theoretical work demonstrated that Majorana Ising spin is a manifestation of symmetry-protected topology, where the spin direction is governed by crystalline symmetries.[11,15]

Intrinsic TRI class DIII TSCs are experimentally scarce due to the stringent requirement for odd-parity pairing in the presence of time-reversal symmetry. Consequently, theoretical research has identified systems exhibiting strong spin–orbit coupling (SOC) as promising candidates for engineering these topological phases. Key proposed platforms include doped topological insulators such as $Cu_xBi_2Se_3$,[18] topological insulator thin films sandwiched between $s_\pm$-wave superconductors with opposite pairing phases,[19] and bilayers featuring linear and cubic Rashba SOCs.[20,22] Additionally, Rashba monolayers proximity-coupled to extended s-wave superconductors (such as iron-based superconductors) offer a high-temperature pathway to this state.[21] Despite these theoretical advances, the manipulation of the Majorana Ising spin — the anisotropic magnetic response of the helical edge modes — via the direct electrical tuning of SOC parameters in 2D class DIII TSCs remains largely unexplored.

This work presents a comprehensive investigation into the orientation and tunability of Majorana Ising spins within TRI TSCs engineered in two-dimensional (2D) spin–orbit coupled systems proximitized to an extended s-wave superconductor. We demonstrate that the interplay between Rashba and Dresselhaus SOCs plays a decisive role in determining the Ising spin orientation. In the limit of pure Rashba SOC, the Ising spin aligns along the x-axis, protected by mirror symmetry M_x. In the limit of pure Dresselhaus SOC, it orients along the y-axis, protected by the combined rotational-mirror symmetry C_{2y}. Most crucially, we reveal that when both interactions coexist, the Ising spin direction becomes continuously tunable within the basal plane. By adjusting the relative strengths of the SOC parameters — experimentally accessible via gating in semiconductor heterostructures — any orientation between the x- and y-axes can be achieved. We validate these findings by calculating the topological winding number W and elucidating the symmetry-protection mechanism for the tunable phases. These results propose a viable pathway for manipulating Majorana fermions in quantum devices through purely electrical means, bridging the gap between symmetry-protected topology and functional spintronic applications.

2. Model

We construct a minimal 2D tight-binding model on a square lattice to investigate class DIII TSCs driven by SOC and extended s-wave pairing. The corresponding normal-state Hamiltonian in momentum space is given by

$$h(\boldsymbol{k}) = -2t(\cos k_x + \cos k_y) + h_{\mathrm{SOC}}, \tag{1}$$

where t denotes the nearest-neighbor hopping amplitude. The term h_{SOC} encapsulates the SOC interactions, including both Rashba and Dresselhaus types, which are particularly relevant for systems such as (110)-grown semiconductor heterostructures.[23] In this work, we examine specific isotropic and anisotropic variants of Rashba and Dresselhaus SOCs,[24] which are summarized in Table 1. The spin textures on the Fermi surface for these four SOC configurations are illustrated in Fig. 1.

Superconductivity is induced in this spin–orbit coupled system via the proximity effect. The system is described by the Bogoliubov–de Gennes (BdG) Hamiltonian $\mathcal{H} = \frac{1}{2}\sum_{\boldsymbol{k}} \Psi_{\boldsymbol{k}}^\dagger \mathcal{H}_{\mathrm{BdG}} \Psi_{\boldsymbol{k}}$, where the basis function is defined as $\Psi_{\boldsymbol{k}}^\dagger = (c_{\boldsymbol{k},\uparrow}^\dagger, c_{\boldsymbol{k},\downarrow}^\dagger, c_{-\boldsymbol{k},\uparrow}, c_{-\boldsymbol{k},\downarrow})$, and

$$\mathcal{H}_{\mathrm{BdG}} = \begin{pmatrix} h(\boldsymbol{k}) - \mu & \Delta \\ \Delta^\dagger & -h^*(-\boldsymbol{k}) + \mu \end{pmatrix}. \tag{2}$$

The off-diagonal pairing potential, $\Delta = [\Delta_0 + 2\Delta_1(\cos k_x + \cos k_y)]s_y$, corresponds to an $s_\pm$-wave superconducting pairing.

Table 1. Explicit form of isotropic and anisotropic Rashba and Dresselhaus SOCs.

	Rashba SOC	Dresselhaus SOC
Isotropic	$-\sin k_y s_x + \sin k_x s_y$	$\sin k_x s_x + \sin k_y s_y$
Anisotropic	$\sin k_y s_x + \sin k_x s_y$	$\sin k_x s_x - \sin k_y s_y$

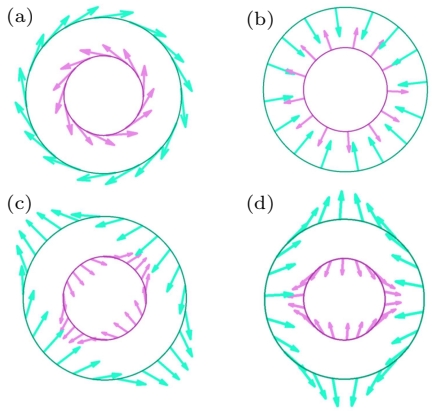


Fig. 1. Spin textures of distinct SOC types on the Fermi surface. (a) and (b) illustrate the spin textures for isotropic Rashba and Dresselhaus SOC, respectively. (c) and (d) correspond to the anisotropic cases.

For the case of isotropic Rashba SOC, the proximity effect induces $s_\pm$ pairing within the Rashba layer. A critical condition arises if the Rashba spin-splitting is sufficiently large that the inner and outer helical Fermi surfaces intersect regions of the Brillouin zone with opposite signs of the induced superconducting gap. This condition is met when the nodal ring of the pairing function lies between the inner and outer Fermi surfaces. In this regime, a TRI helical p-wave superconducting phase, characterized by a $\mathbb{Z}_2$ invariant, is realized.[21] While the other three SOC variants exhibit distinct spin textures, they all support a helical p-wave superconducting phase, provided that the two helical Fermi surfaces experience opposite signs of the induced gap. Consequently, we investigate the Majorana Ising spin for TRI TSCs arising from these four distinct SOC configurations.

3. Properties of the Ising spin

As mentioned previously, in spinful superconductors, the Majorana Ising spin character has been demonstrated to result from symmetry-protected topological phases.[15] Furthermore, for a pairing potential with a given irreducible representation, the crystal symmetry uniquely determines the direction of the Majorana Ising spin.[25] This provides a theoretical foundation for utilizing magnetic fields to probe electron pairing behaviors in superconducting materials. In this section, we demonstrate that for a given pairing potential, the Majorana Ising spin also responds differently to distinct SOCs. Specifically, in the presence of Rashba SOC, the Ising spin aligns along the x-axis, while under Dresselhaus SOC, it orients along the y-axis. This leads to the key observation that the Majorana Ising spin's orientation can be continuously controlled in-plane by tuning the relative strength between the two SOC types.

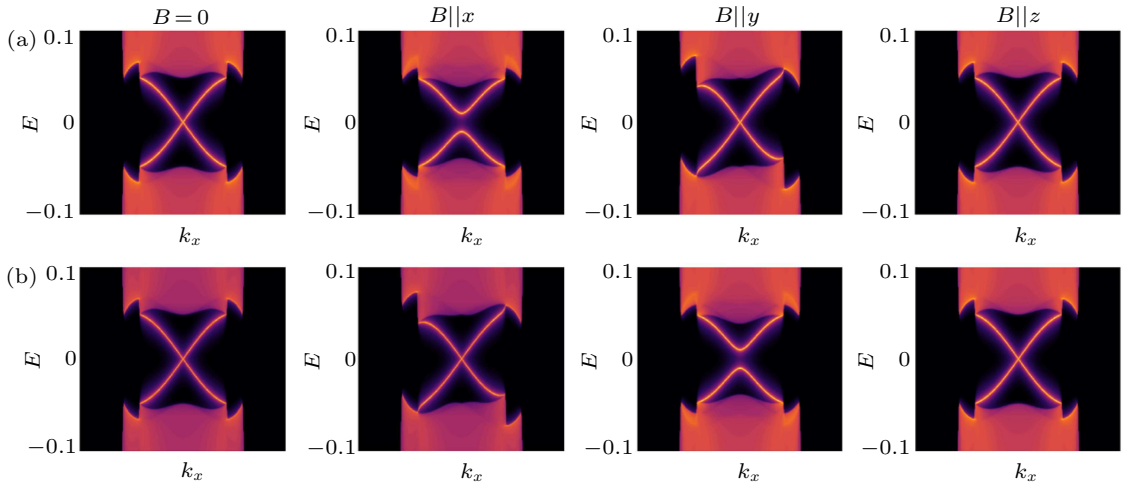


Fig. 2. Evolution of the edge states under a magnetic field ($B = 0.01$) for the four SOCs in Eq. (2), with a y-direction open boundary. The edge states are identical for isotropic and anisotropic conditions in both the (a) Rashba-type ($\alpha_R = 0.5$) and (b) Dresselhaus-type ($\alpha_D = 0.5$) SOCs. Common parameters, $t = 1$, $\mu = -2$, $\Delta_0 = 0.2$, $\Delta_1 = -0.1$.

Figures 2(a)–2(d) illustrate the evolution of edge states with respect to the magnetic field direction for the four different SOC types, assuming open boundary conditions along the y-direction. At zero magnetic field, the system exhibits a Kramers pair of helical Majorana edge modes for all four SOC cases. For both isotropic and anisotropic Rashba SOC, the MKPs respond exclusively to a magnetic field applied along the x-direction, resulting in a gap opening for the Majorana zero modes at $k_x = 0$. In contrast, for the Dresselhaus SOC cases, the MKPs are responsive only to a y-directed magnetic field. In a TRI topological superconducting phase, Majorana zero modes generally remain gapless when the magnetic field is oriented perpendicular to the Ising spin direction; a gap opens only when the field has a component parallel to the Ising spin axis. Based on this principle, the distinct directional selectivity observed in our calculations implies the orientation

of the Ising spin: it is aligned along the x-axis for both forms of Rashba SOC and along the y-axis for both forms of Dresselhaus SOC. We next calculate the topological invariant to characterize this topological phase.

4. Topological invariant

This Majorana Ising spin character defines a symmetry-protected topological phase. The corresponding symmetry analysis for the four SOC cases is summarized in Table 2. Under time-reversal symmetry, our analysis indicates that the Ising spin is protected by mirror symmetry M_x for Rashba-type SOC and by rotational symmetry C_{2y} for Dresselhaus-type SOC. These conclusions are valid for both isotropic and anisotropic SOC.

Table 2. Symmetries protecting the Ising spin and their operator forms in different SOC systems, where τ_i $(i=1,2,3)$ denote the Pauli matrices acting in the particle–hole space.

Type of SOC	Symmetry	Operator
Isotropic/anisotropic Rashba	M_x	$\mathrm{i}\tau_z s_x$
Isotropic/anisotropic Dresselhaus	C_{2y}	$\mathrm{i}\tau_0 s_y$

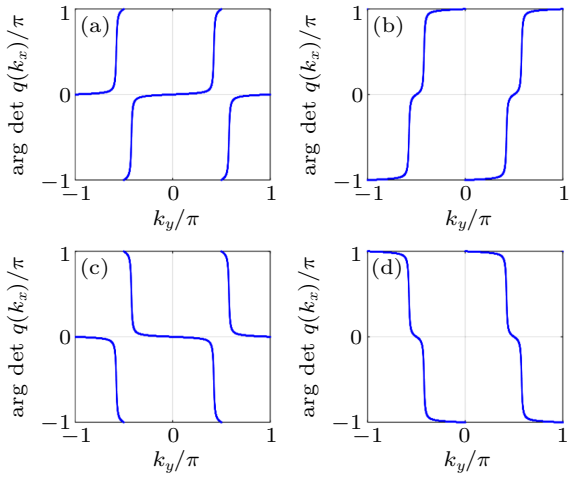


Fig. 3. Winding of $\arg\det q(k_x)$ for each SOC. (a), (c) For Rashba-type SOC: $\alpha_R = 0.5$, isotropic $W = 2$ and anisotropic $W = -2$. (b), (d) For Dresselhaus-type SOC: $\alpha_D = 0.5$, isotropic $W = 2$ and anisotropic $W = -2$. Common parameters, $t = 1$, $\mu = -2$, $\Delta_0 = 0.2$, $\Delta_1 = -0.1$.

The effective chiral symmetry operator, denoted as Γ, is constructed from the original chiral operator $\gamma = -\mathrm{i}\tau_x s_y$ and is defined by the following relation: $\Gamma_{M_x} = \tau_y s_z$, $\Gamma_{C_{2y}} = \tau_x s_0$, $\Gamma_{M_x} = \tau_y s_z$, and $\Gamma_{C_{2y}} = \tau_x s_0$. Using Γ, we compute the winding number at the TRI momentum $k_x = 0$,

$$W[\Gamma, y] = \int_{-\pi}^{\pi} \frac{\mathrm{d}k_y}{2\pi} \frac{\partial}{\partial k_y} \arg\det q(k_x), \tag{3}$$

where $W[\Gamma, y]$ is the winding number corresponding to Majorana edge states on the (010) edge, and $q(k_x)$ is defined as the off-diagonal component of the Hamiltonian (Eq. (2)) in the chiral basis. By the bulk–boundary correspondence under the effective chiral symmetry Γ, a nonzero winding number implies protected zero-energy boundary modes. In the present TRI setting, the boundary zero modes appear as an MKP, i.e., two Majorana modes related by TRS. The results in Fig. 3 show that for all cases, the winding number is nonzero ($W = \pm 2$). Specifically, the result $|W| = 2$ provides topological verification of the Majorana Kramers pairs on the (010) edge, linking the symmetry protection directly to the existence of the edge states.

5. Coexisting Rashba and Dresselhaus SOCs

Following the preceding discussion on the distinct effects of Rashba and Dresselhaus SOC, a natural question arises: how does the Ising spin orientation evolve when both types of SOC are present? For simplicity, we restrict this section to the isotropic forms of linear Rashba and Dresselhaus SOC. The direction of the Majorana Ising spin determines a highly anisotropic magnetic response. To investigate this directionality intuitively, we study the magnetic-field-induced quasiparticle gap in the edge-state spectrum, as shown in Figs. 4(a) and 4(b). Consistent with our previous conclusions, when only Rashba SOC is present, the Ising spin aligns along the x-direction, whereas it aligns along the y-direction for pure Dresselhaus SOC. Our investigation reveals that when Rashba and Dresselhaus SOC coexist with equal strength, the Majorana Ising spin orients along the diagonal direction in the x–y plane (Fig. 4(c)). Furthermore, varying their relative strength enables continuous rotation of the Ising spin within the plane (Figs. 4(a)–4(d)).

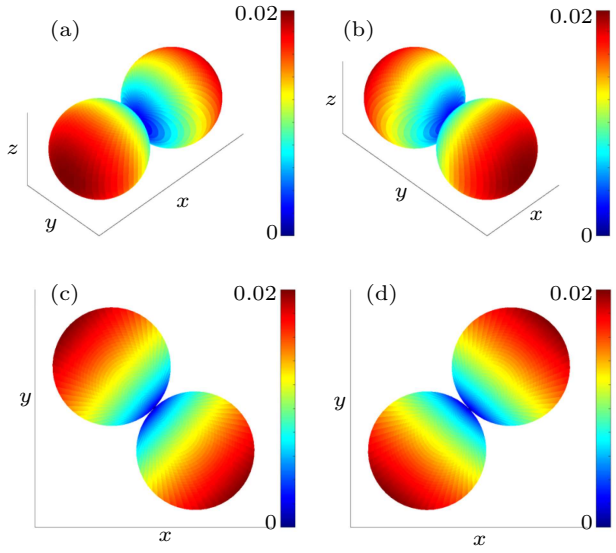


Fig. 4. Magnetic-field-induced ($B = 0.01$) quasiparticle gap in the edge-state spectrum. (a) For pure Rashba SOC ($\alpha_R = 0.5, \alpha_D = 0$). (b) For pure Dresselhaus SOC ($\alpha_D = 0.5, \alpha_R = 0$). The case of mixed Rashba and Dresselhaus SOC is depicted in (c) and (d), corresponding to a ratio of $\alpha_R/\alpha_D = 1$ for (c) and $\alpha_R/\alpha_D = -1$ for (d). Common parameters: $t = 1, \mu = -2.0, \Delta_0 = 0.2, \Delta_1 = -0.1$.

To understand the physical origin of this continuous rotation, it is necessary to address the role of crystalline symmetry. Conventionally, for a given pairing symmetry, the orientation of the Majorana Ising spin is uniquely fixed by the crystal

symmetries protecting the topological phase.[25] This principle strictly governs the limiting cases in our model: the pure Rashba case is protected by mirror symmetry M_x, pinning the spin to the x-axis, while the pure Dresselhaus case is protected by rotation symmetry C_{2y}, pinning it to the y-axis.

However, in the mixed regime where both SOCs coexist, these global spatial symmetries are explicitly broken. With the rigid symmetry constraints lifted, the orientation of the Majorana Ising spin is no longer pinned to a specific crystallographic axis. Instead, it is determined by the direction of the effective spin–orbit field experienced by the electrons at the Fermi momentum. This effective field behaves as the vector sum of the Rashba and Dresselhaus components. As the relative strength α_R/α_D is varied electrically, the direction of this resultant vector rotates continuously within the basal plane. Consequently, the Majorana Ising spin tracks this effective quantization axis, allowing for the continuous tunability of the magnetic response.

6. Discussion and conclusion

In this work, we have demonstrated that in systems with Rashba or Dresselhaus SOC, the Majorana Ising spin can orient along different directions even under the same pairing potential. Through symmetry analysis, we have established that for Rashba-type SOC, the Ising spin aligns along the x-axis on the (010) edge, protected by mirror symmetry M_x. We derived the corresponding effective chiral operator and calculated the resulting winding number to be 2 for the isotropic case and -2 for the anisotropic case. Similarly, for Dresselhaus-type SOC, the Ising spin orients along the y-axis, protected by rotational symmetry C_{2y}, with winding numbers of 2 (isotropic) and -2 (anisotropic).

Crucially, we revealed that when Rashba and Dresselhaus SOC coexist, the relative strength between them dictates the in-plane orientation of the Majorana Ising spin. In this mixed regime, the global crystalline symmetries (M_x and C_{2y}) are explicitly broken, lifting the rigid symmetry constraints on the spin direction. Consequently, the Majorana Ising spin continuously tracks the effective spin–orbit magnetic field vector — determined by the vector sum of the SOC fields — as the ratio is tuned. This insight extends the theoretical framework of symmetry-protected topology and offers valuable perspectives for probing electronic pairing behaviors through magnetic-field tuning.

To experimentally realize the tunable Majorana Ising spin predicted in our model, we propose a heterostructure based on a 2D InSb or InAs quantum well grown along the (110) direction, proximity-coupled to an iron-based superconductor (e.g., Fe(Te,Se) or LiFeAs). Iron-based superconductors are particularly suitable candidates as they naturally provide the extended s-wave pairing symmetry[26–28] assumed in our model, combined with a high superconducting critical temperature. Furthermore, the regime of comparable Rashba and Dresselhaus strengths $\alpha_R \approx \alpha_D$ is experimentally accessible. The feasibility of tuning α_R to match α_D has been rigorously demonstrated in the observation of the persistent spin helix state,[29–32] confirming that the ratio α_R/α_D can be precisely controlled to rotate the Majorana Ising spin orientation.

While electrostatic gating offers a theoretical pathway to tune the SOC ratio, we acknowledge that practical implementation faces challenges from interface disorder and band hybridization. To enhance experimental robustness, we propose two specific material strategies. First, epitaxial heterostructures are essential for reducing disorder. Unlike evaporated contacts, interfaces grown via *in-situ* molecular beam epitaxy (MBE) — such as Fe-based thin films on (110)-InAs quantum wells — demonstrate a "hard" superconducting gap, indicating a ballistic interface free from disorder-induced subgap states.[23] Second, to mitigate strong band hybridization (metallization) that might screen the gate electric field, van der Waals (vdW) heterostructures offer a distinct advantage. By stacking 2D semiconductors onto layered superconductors (e.g., Fe(Te,Se) flakes), one creates atomically sharp interfaces without dangling bonds. This minimizes the renormalization of the semiconductor's parameters, ensuring that the SOC coefficient remains effectively tunable by external gates. Additionally, the use of semi-insulating substrates (such as $SrTiO_3$) is recommended to eliminate parasitic bulk conduction that could otherwise obscure the transport signatures.

Finally, we discuss how the electrical rotation of the Majorana Ising spin can be detected in experiments. We propose angle-dependent tunneling spectroscopy as the primary detection method. The defining feature of the Majorana Ising spin is its anisotropic response to magnetic fields: the Majorana edge modes remain gapless only when the magnetic field is perpendicular to the Ising spin polarization; a parallel field opens a gap. Experimentally, this can be probed by measuring the differential conductance ($\mathrm{d}I/\mathrm{d}V$) using a tunnel probe. At zero magnetic field, the Majorana modes manifest as a zero-bias conductance peak (ZBCP). By applying an in-plane magnetic field of fixed magnitude and rotating its angle θ, the ZBCP will split into two finite-energy peaks only when the field aligns with the Ising spin direction (the "hard axis"). Crucially, as the SOC ratio α_R/α_D is tuned via electrical gating, the angle θ at which this splitting is maximal will shift continuously. This angle-dependent evolution of the spectral gap serves as a direct observable quantity reflecting the rotation of the Ising spin.

Acknowledgements

This work was supported by the National Natural Science Foundation of China (Grant Nos. 12474151, 92565103, and 12547101). D.-H.X. also acknowledges the Beijing National Laboratory for Condensed Matter Physics (Grant No. 2024BNLCMPKF025) and the Fundamental Research Funds for the Central Universities (Grant No. 2025CDJ-IAISYB-032).

References

[1] Hasan M Z and Kane C L 2010 *Rev. Mod. Phys.* **82** 3045
[2] Qi X L and Zhang S C 2011 *Rev. Mod. Phys.* **83** 1057
[3] Sato M and Ando Y 2017 *Reports on Progress in Physics* **80** 076501
[4] Nayak C, Simon S H, Stern A, Freedman M and Das Sarma S 2008 *Rev. Mod. Phys.* **80** 1083
[5] Altland A and Zirnbauer M R 1997 *Phys. Rev. B* **55** 1142
[6] Read N and Green D 2000 *Phys. Rev. B* **61** 10267
[7] Schnyder A P, Ryu S, Furusaki A and Ludwig A W W 2008 *Phys. Rev. B* **78** 195125
[8] Alicea J 2012 *Reports on Progress in Physics* **75** 076501
[9] Nagato Y, Higashitani S and Nagai K 2009 *J. Phys. Soc. Jpn.* **78** 123603
[10] Chung S B and Zhang S C 2009 *Phys. Rev. Lett.* **103** 235301
[11] Mizushima T, Sato M and Machida K 2012 *Phys. Rev. Lett.* **109** 165301
[12] Sato M and Fujimoto S 2009 *Phys. Rev. B* **79** 094504
[13] Mizushima T and Machida K 2011 *J. Low Temp. Phys.* **162** 204
[14] Shindou R Furusaki A and Nagaosa N 2010 *Phys. Rev. B* **82** 180505
[15] Shiozaki K and Sato M 2014 *Phys. Rev. B* **90** 165114
[16] Silaev M A 2011 *Phys. Rev. B* **84** 144508
[17] Yada K, Sato M, Tanaka Y and Yokoyama T 2011 *Phys. Rev. B* **83** 064505
[18] Fu L and Berg E 2010 *Phys. Rev. Lett.* **105** 097001
[19] Liu C X and Trauzettel B 2011 *Phys. Rev. B* **83** 220510
[20] Nakosai S, Tanaka Y and Nagaosa N 2012 *Phys. Rev. Lett.* **108** 147003
[21] Zhang F, Kane C L and Mele E J 2013 *Phys. Rev. Lett.* **111** 056402
[22] Xu Q S, Wang Z M, Chen C Z, Hu L H, Wang R and Xu D H 2026 *Phys. Rev. B* **113** L161404
[23] Alicea J 2010 *Phys. Rev. B* **81** 125318
[24] Simon E, Szilva A, Ujfalussy B and Lazarovits B, Zarand G and Szunyogh L 2010 *Phys. Rev. B* **81** 235438
[25] Xiong Y, Yamakage A, Kobayashi S, Sato M and Tanaka Y 2017 *Crystals* **7** 58
[26] Mazin I I, Singh D J, Johannes M D and Du M H 2008 *Phys. Rev. Lett.* **101** 057003
[27] Kuroki K, Onari S, Arita R, Usui H, Tanaka Y, Kontani F H and Aoki H 2008 *Phys. Rev. Lett.* **101** 087004
[28] Hanaguri T, Niitaka S, Kuroki K and Takagi H 2010 *Science* **328** 474
[29] Koralek J D, Weber C P, Orenstein J, Bernevig B A, Zhang S C, Mack S and Awschalom D D 2009 *Nature* **458** 610
[30] Walser M P, Reichl C, Wegscheider W and Salis G 2012 *Nat. Phys.* **8** 757
[31] Kohda M, *et al*. 2012 *Phys. Rev. B* **86** 081306
[32] Sasaki A, *et al*. 2014 *Nat. Nanotech.* **9** 703
[33] Chang W, *et al*. 2014 *Nat. Nanotech.* **10** 232